Prediction of the Process of a Slowly Moving Loess Landslide by Electrical Resistivity Tomography

Sándor Szalai, Ernő Prácser, Kitti Szokoli, and Ádám Tóth

Abstract

A slowly moving loess landslide along the River Danube in South Hungary was studied using electrical resistivity tomography (ERT). The aim of the research was to determine the fracture system of the study site. It seems to be the only possibility to get information about the landslide and its further evolution due to the homogeneous composition of the loess. The mass movement was expected to occur in the direction of the identified crack openings. The applicability of the ERT technique for such a supposedly dense fracture system was studied by numerical modelling and the results have been verified in the field. It was shown that it is especially important to carry out the field measurements following dry periods; otherwise the interpretation may become extremely difficult if not impossible. The dip of the fractures could not be observed and they could not be explored deeply. It was possible to map their surface projection to get the desired information about the structure of the landslide. Fracture zones could be especially well localized enabling the prediction of the positions of future rupture surfaces and thus also the delineation of the endangered zone. Although the area outside of the one that already subsided is not endangered yet, the area which has already started to move is going to break into two. Parts of the about 5 m wide blocks at the front of the landslide may fall or slide down anytime. The area below the buildings was assumed to move as one unit. Most of our predictions have been verified by the mass movements which occurred about one and half years after the measurements. The ERT method proved to be a good tool to characterize the fracture system of such a landslide area, enabling the prediction of future rupture surfaces and also delineation of the endangered area. Its use is therefore highly recommended to monitor landslides.

Keywords

Loess landslide • Electric resistivity tomography • Prediction • Slowly moving landslide • Fracture

S. Szalai (✉) · E. Prácser · K. Szokoli
MTA CSFK GGI, Csatkay u. 6-8, Sopron, 9400, Hungary
e-mail: szalai@ggki.hu

E. Prácser
e-mail: pracser@ggki.hu

K. Szokoli
e-mail: szk@ggki.hu

Á. Tóth
Eötvös Loránd University, Budapest, Hungary
e-mail: adam.geophysics@gmail.com

Introduction

A landslide is a down slope movement of soil or rock which occurs due to gravity, local geological and groundwater conditions, extreme weather events, earthquakes and other factors (e.g. Cruden and Varnes 1996). Landslides can cause extreme damage to facilities, roads, and human life (Guzzetti et al. 2012). Therefore mapping them is important for hazard

M. Mikoš et al. (eds.), *Advancing Culture of Living with Landslides*,
DOI 10.1007/978-3-319-53487-9_14

zonation, planning and protection purposes (Booth et al. 2009; Guzzetti et al. 2012).

Loess is widely distributed all over the world (Gallet et al. 1998). Spatial distribution e.g. in Europe is demonstrated in Haase et al. (2007). Landslides frequently take place in loess-covered areas. There are a lot of loess landslides among others in China (Liao et al. 2008; Bai et al. 2012; Li et al. 2012). This type of landslide occurs frequently along the loess cliffs in the Hungarian section of the Danube, as well (Pécsi 1994). One of the loess landslides along river Danube, the Dunaszekcső one, is studied here.

Remote sensing techniques are very significant in studying landslides. Mapping the surface area affected by the landslide is often done by observation of aerial photographs or remote-sensing images (Van Westen 2004; Tofani et al. 2013; Scaioni et al. 2014) which indicate the topographical extent of the landslide. However, if the landslide is ancient or not very active, its morphological features and boundaries may be degraded requiring recognition in depth. Geodetic methods are also distributed in landslide investigations as shown in the example of the site presented in the papers by Újvári et al. (2009) and Bányai et al. (2013). Geophysical methods which can also be very fruitful for studying landslides are summarised by Jongmans and Garambois (2007).

Geolectrical resistivity measurements were carried out in landslide studies among others by Lapenna et al. (2005). A recent review by Loke et al. (2013) details use of ERT to characterize landslides. These techniques aimed to delineate the horizontal and/or vertical boundaries of the sliding volume and their internal characteristics.

Geotechnical tools would be perfect to map fractures but they provide only single points information. In contrast the resistivity method is able to measure a dense fracture system (Szalai et al. 2002; Falco et al. 2013). Bievre et al. (2012) aimed to characterise fissures within a fine-grained landslide using ERT. Jones et al. (2014) mapped desiccation cracks with ERT on a flood embankment.

In the research presented here, the Authors wanted to complement these investigations by studying the fracture system of the Dunaszekcső landslide to allow prediction of future rupture surfaces and thus delineate the most hazardous areas. This knowledge is also important because the continuity and geometry, orientation and dip of the major fractures are crucial information for assessing rock stability and landslide evolution.

Fracture detection in landslide areas is a crucial point because it is a meaningful precursor sign long time before the failure. If the fractures could be localised, the endangered areas could be delineated in time to take precautions. In this article, geological and geomorphological settings of the study area will be presented first and then the use of ERT in fracture system investigations will be demonstrated and finally the field survey results will be validated in situ.

Geology and Former Research in the Area

The study area is in the Baranya Hills, in Hungary (Fig. 1a). Study site Dunaszekcső is seen in the most southern part of the map in Fig. 1b. The bedrock at Dunaszekcső is weakly karstified Triassic–Jurassic limestone identifiable at 200–250 m below the surface (Moyzes and Scheuer, 1978). It is mantled by clayey and sandy sediments formed in the Pannonian s.l. epoch (equivalent to the Upper Miocene and the Pliocene, 12.6 to ~2.6–2.4 Ma; Rónai 1985). The uppermost 70 m of the sediment sequence are sandy and clayey

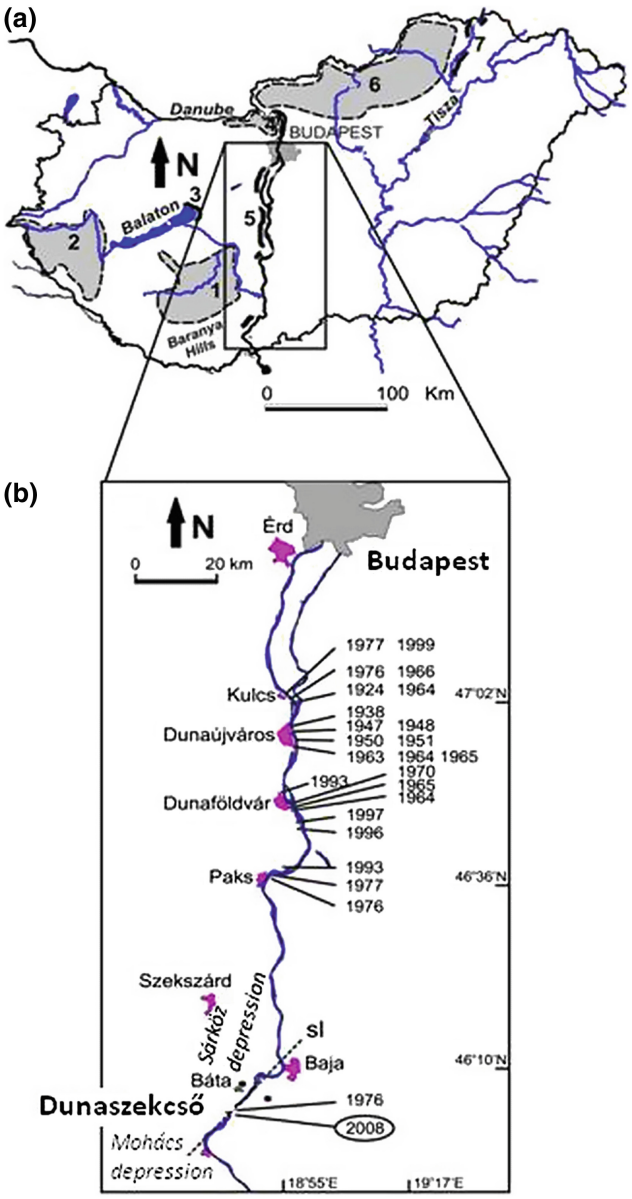

Fig. 1 Study area location. **a** Landslide endangered areas. **b** Large landslides in the 20th century along the high bank of Danube between Budapest and Mohács. Numbers indicate the events which occurred in the past

loess layers with brown to red fossil soils accumulated during the Pleistocene (Fig. 2). The cliff reaches its highest point (142 m a.s.l.) at Vár Hill (Figs. 2 and 3).

The flood plain of the Danube is very narrow or missing at Vár Hill. The bluff consists of a 20–30 m high vertical loess wall above the 10–20 m high slopes that consist of reworked loess from past landslides and fluvial mud, sand and gravel deposits of the Danube (Fig. 2).

The younger loess series on top is prone to collapse, while the older loess below is much more compact (Moyzes and Scheuer 1978). The ground water recharged from percolated rainfall and the Lánka stream resides in the lower part of the young and more porous loess deposits (Fig. 2). Ground water flows to the SE during base flow because of the sucking effect of the Danube (Moyzes and Scheuer 1978).

Field observations show the development of tension cracks in the loess complex parallel as well as perpendicular to the channel of the Danube, indicating reduced rock strength. The vertical cracks are clearly visible on the roof of the Töröklyuk cave, a large natural cavity. Cracking was probably induced by both previous sliding events and recent slumping.

Landslides in the hill region we studied are concentrated in areas where relative relief is sufficiently high. This situation occurs along the Danube bank where stream undercutting has produced relatively high bluffs. One of the most important factors of a landslide is the hydrological condition of high bluffs. The Danube has a water level fluctuation range of nearly 10 m.

Along the steep bank of the Danube, the Upper Pannonian sediment sequence consisting of alternating permeable and impervious layers is exposed in some places below the Pleistocene or Upper Pliocene loess sequence or the Pliocene red clays. Because of previous slumping and lateral erosion by the Danube, the Upper Pannonian sediments are partly redeposited with a disturbed stratification or buried under younger deposits. The Upper Pannonian sand deposits provide confined aquifers, and their water under pressure locally moistens the overlying past slump deposits, favouring the reactivation of existing slumps and the generation of new landslides. During spring–summer floods, the river inundates the surface, leading to the rise of the local groundwater table. This circumstance is noteworthy because slumps and earth slides tend to take place after prolonged high-water stages of the Danube (Fábián et al. 2006).

The Dunaszekcső landslide is termed as a slow earth slide following the classification of Cruden and Varnes (1996). According to USGS classification (Highland 2004), the landslide could also be defined as block slide.

The study site is close to the edge of the landslide (Fig. 3). At the time of the measurements, in November 2013, one

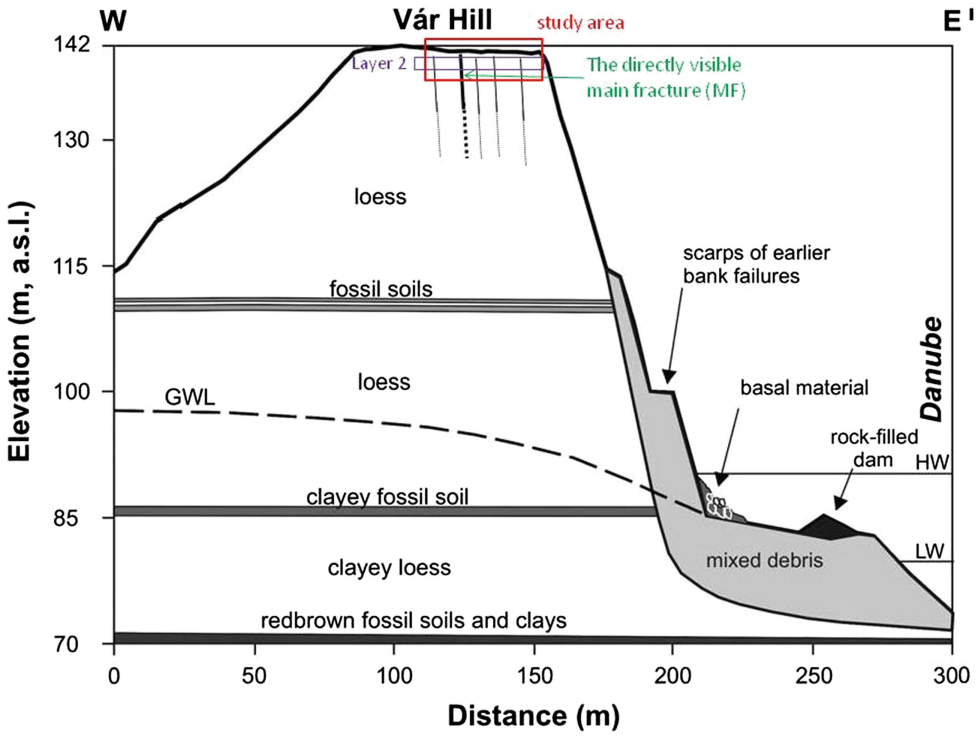

Fig. 2 Geological cross-section of the high bank at Dunaszekcső (after Moyzes and Scheuer 1978). Vertical exaggeration: ×3. *GWL* ground water level (in July 2008), *HW* highest water, *LW* lowest water

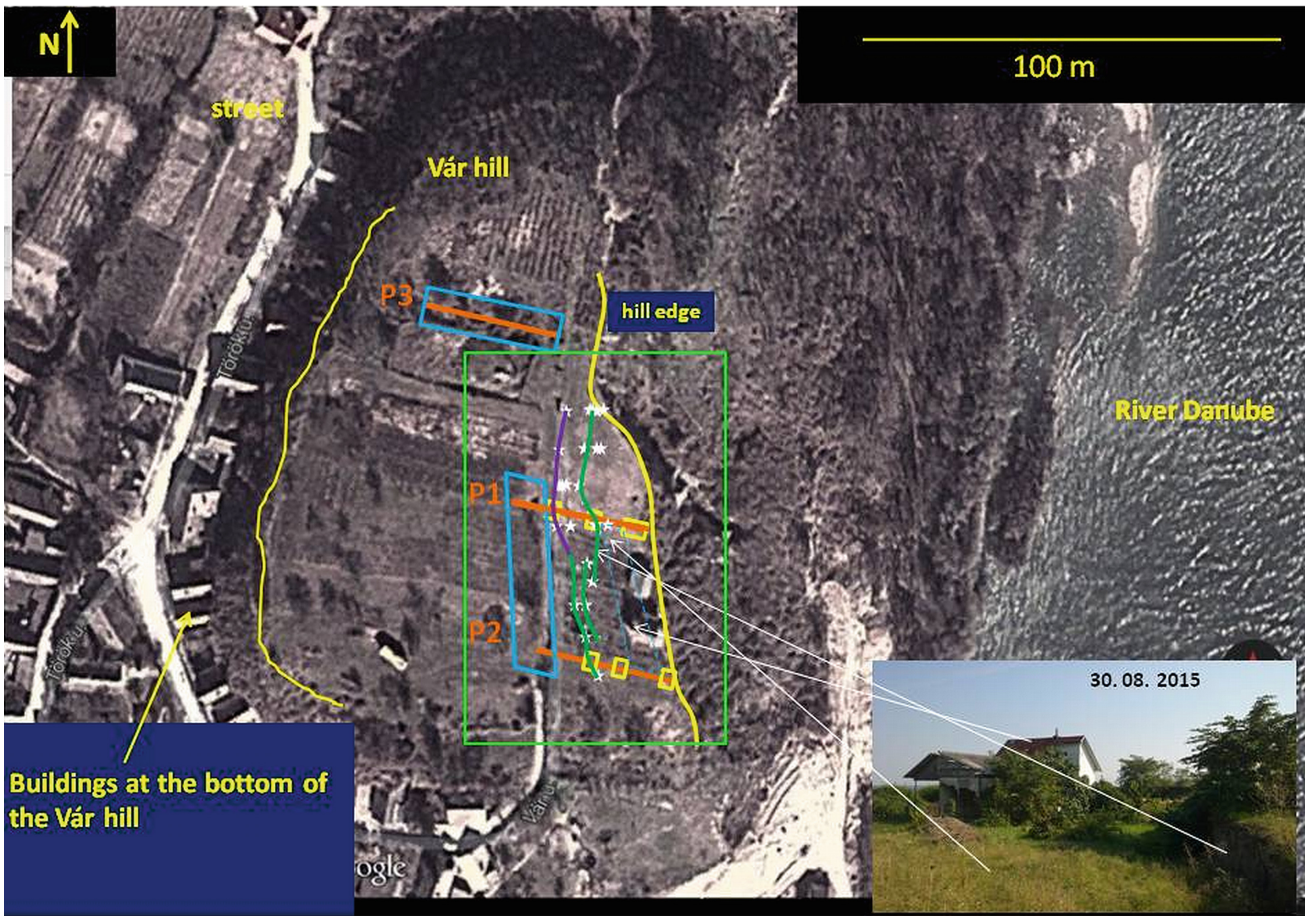

Fig. 3 Google map of the study site. ERT profiles P1, P2 and P3 (*brown lines*); the main fracture (MF) visible at the time of the measurements (*purple curve*); new fractures developed after the measurements (*green curves*); the actual scarp (*yellow curve*); fracture positions (*white stars*); fracture zones in the ERT section (*yellow rectangle*). The photo in the *lower right corner* was made from the north after the new mass movements. The *light green rectangle* denotes the area shown in Fig. 5

fracture was visible. Since many fractures formed, we know that the fractures reach very close to the surface. They are hidden by grass and about 5–10 cm thick soil (we explored many of them) and they seem to go down at least 1–2 m. Close to the surface most of the fractures are about 3–5 cm wide. There had not been any rainfall for the previous three weeks and all fractures which were dug out were dry.

Investigation Method

Since the resistivity method has successfully been used to characterise fractures, we decided to use Electric Resistivity Tomography (ERT). In this study a Wenner-Schlumberger (W-S) system has been used. The W-S array is the most sensitive configuration to detect changes in vertical resistivity.

Field Study—Dunaszekcső, Hungary

The Field Measurement

All profiles were acquired in November 2013. A 72 electrode Syscal Pro Standard & Switch system was used for the field measurements with 0.5 m electrode spacing which gives an image up to 7.2 m deep.

Three electrical profiles were conducted on the site (labelled P1–P3) whose locations are given in Fig. 3.

They are closely perpendicular to the slope. Profile 1 (P1) is in the middle of the investigated area which supposed to be the most characteristic for the landslide because there is already a visible fracture here which we called main fracture (MF, in Fig. 3). The largest part of P2 is in the area between the expected elongation of the MF and the edge of the

landslide, although the MF does not reach it. P3 is on the other side of the supposed northern elongation of the MF. Therefore the expected order of the fracturing and that of the danger of the areas is below P1, P2 and P3, respectively. Data were inverted using Earthlmager 2D.

Field Activities: Results and Discussion

The field results are summarised in Fig. 4. The interpretation is demonstrated in the example of P1 (Fig. 4b). The green areas in the inhomogeneous layer at a depth of 0.5–2.0 m from the surface (layer 2), with resistivity values about 150 Ωm have been regarded as background and are assumed to describe dry loess. The more conductive uppermost layer with a resistivity of 70–100 Ωm (layer 1, from the top down to 0.5 m) is supposed to be a little more humid loess likely due to the low amount of rain before the measurements. The conductive layer (below 50 Ωm) in the bottom of the section (below 2.5 m, layer 3) has to be even more humid loess. (This layer is not well seen in the presented shallow sections.) The water from earlier rainfalls seems to have not yet disappeared from here. The resistivity of humid loess is in the range of 20–50 Ωm (Caicedo et al. 2013) but fractures may even further decrease its resistivity by increasing the relative volume of the water.

To achieve our goal to describe fractures, we concentrated to the non-continuous middle layer 2. On basis of numerical modelling results in this layer, the effect of the fractures are expected to be seen best. The green zones (about 150 Ωm) are interrupted here by yellow (about 200 Ωm) and red (over 500 Ωm) zones. The yellow/red zones are interpreted as fractures or fracture zones. It is expected that the higher the resistivity value is, the wider a fracture is.

On the P1 section (Fig. 4b) beside the known main fracture (MF, fracture zone 3) at 12–13 m there are two zones in

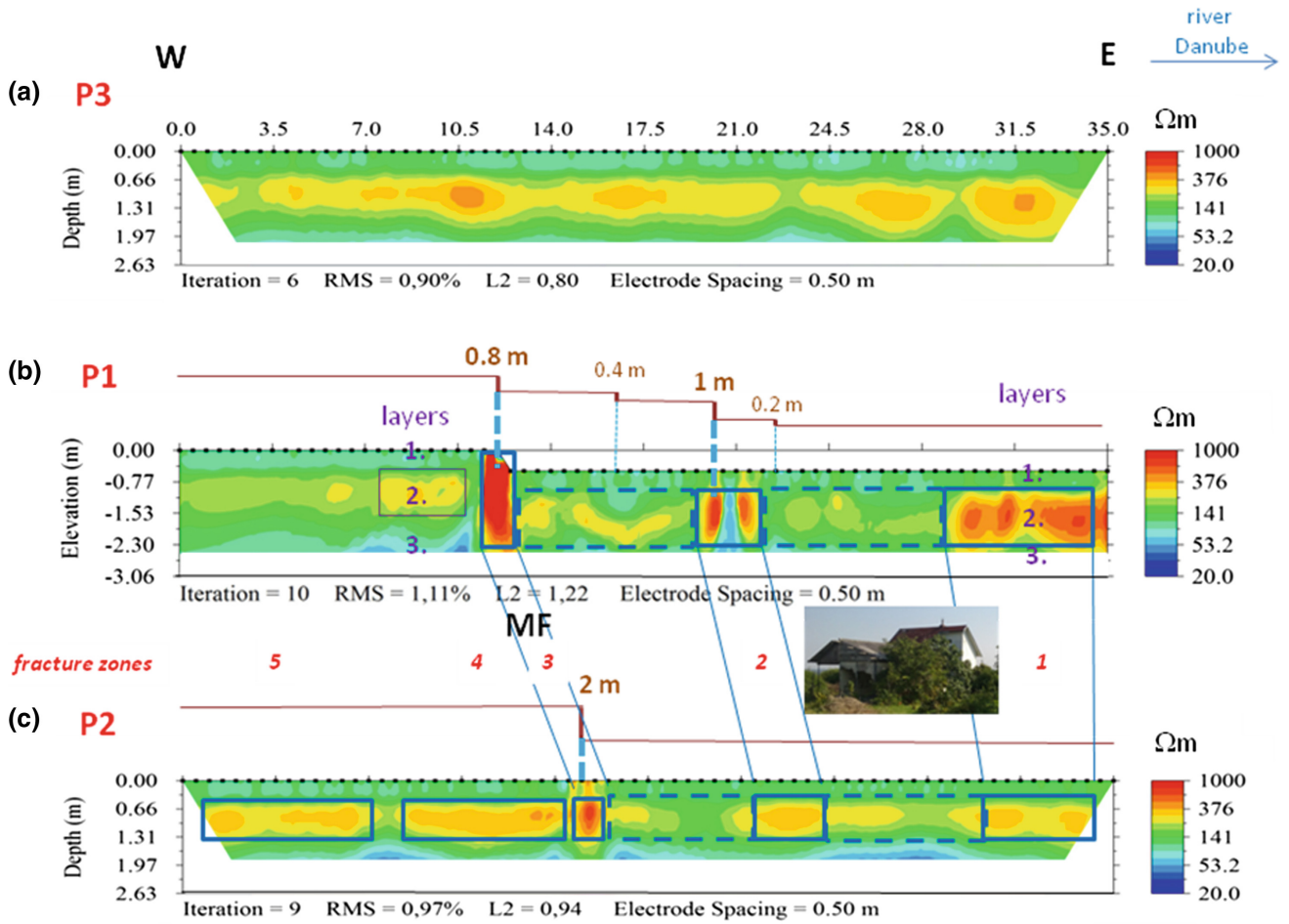

Fig. 4 All ERT profiles. **a** P3 section; **b** P1 section; **a** P2 section. Fracture zones whose resistivity values are significantly larger than the background value in the same depth level (*continuous line rectangles*); fracture-free zones (*dotted line rectangles*); borders of the fracture zones which are predicted to correlate (*blue lines*). Predicted fractures (*thick dotted blue line*); not predicted fractures (thin dotted blue line). Above the P1 and P2 sections their topography and the vertical offset at the fractures on 31. 08. 2015

this "layer" where the resistivity values are significantly greater than the background value: in the 19.5–21.5 m (fracture zone 2) and 28.5–35 m (fracture zone 1) zones.

These fracture zones are well separated from each other. Zone 1, which is closer to the scarp, shows that the loess is very fragmented at the hill edge. Fracture zone 3, whose anomaly value is the largest, belongs to the main fracture (MF) which is directly visible on the surface. Fracture zone 2 is in the middle between zone 1 and zone 3. The consolidated area between zone 1 and zone 3 is likely going to break here. Since fracture zone 1 is fully fractured, its fragments may slide or fall down anytime.

It is important to note that the areas between the fracture zones are less resistive, apparently more solid mechanically than the area west of the MF. The structure of the eastern part may be like this because here the largest part of the mechanical tension might be relaxed in the fracture zones. In the western area at the same time the tension is still almost equally distributed throughout the area. The tension seems therefore to be present everywhere in the hill which is most likely due to its steep topography (Fig. 2).

The area below P2 (Fig. 3) is assumed to be more consolidated (Fig. 4c); the MF has not reached it yet. The resistivity values of all "layers" are in the same range as in the P1 section and also the structure of the section is very similar to that of P1.

They display three very characteristic fracture zones. Fracture zone 1 is at the edge of the slide, zone 2 is in the middle of this zone and zone 3. The very high value of zone 3 lets us assume that the MF crosses P2 here even if it is not seen yet. In this profile fracture zones also seem to appear west of these zones. In the area below P2, the structure is very different between zones 1 and 3 and between zones 4 and 5. While in zones 1–3 there are long fracture-free zones between the fracture zones; in zones 4–5 there are only very short fracture-free zones.

Positioning of individual fractures is only possible if their anomalies are sharp but it was rare in the study area.

The site along P3 (Fig. 4a) seems to be the less endangered among those that were investigated. There is not any indication on the surface of the presence of any fractures. The resistivity sections display a rather homogeneous area. Fractures are supposed to be throughout P3 but they are mostly weak ones. At the end of the profile, the fracture zone 30–33 m was assumed to be mechanically weaker.

The similarity of P1 and P2 sections is remarkable. Most likely both of them contain the fracture zone of the MF and two zones east of it. The western side of the MF is not as structured as the eastern one. The situation is the same for the whole length of P3 although it is also weakly structured containing zones where the resistivity is a little higher than elsewhere along the profile. We suppose that strong structuring (occurrence of zones which are characteristically different from other parts of the profile) develops due to the break of the loess unit at certain locations (producing the fracture zones) and a relaxation in others following it (producing the fracture-free zones). Therefore we supposed that only the well structured area east of the MF between P1 and P2 is actually endangered (Figs. 3 and 4).

Fracture zone 3 in P2 most likely contains the fracture which is visible in P1. Fracture zone 2 which appears on both P1 and P2 profiles was assumed to cover a significant fracture which may develop to a rupture surface. Fracture zones 1 of P1 and P2 also refer to the existence of significant fractures. The relative stability of the area between fracture zones 1 and 2 lets us assume that the buildings which are in this area may sink without serious damage. Due to the lack of well-defined fracture zones the area covered by P3 is not considered to be endangered either. The smaller fractures west of the MF below P1 and P2 and all along P3 may emerge in the first line because of the steep topography of the hill.

Summarising the field results: (1) the field measurements enabled us to divide the homogeneous loess area into three layers. The effect of the fractures can be the best seen in the intermediate layer. (2) Fractured and fracture-free areas proved to be easily distinguishable while individual fractures could not always be separated. (3) The resolution of the measurements could be further improved by decreasing the electrode spacing. (4) The fractures could not be followed in the lowest layer. (5) ERT results enabled us to describe the inner structure of the landslide area. The endangered area could be delineated and even the position(s) of future rupture surfaces could be forecast.

In Situ Validation

The best verification of our results has been given by new movements since our measurements and data interpretation. The movements started very slowly but they accelerated in spring and summer 2015. The actual condition of the study site can be seen in Figs. 3 and 5. They show that the MF continued and now crosses P2 in fracture zone 3 where it was expected on the basis of our study. A new large fracture appeared in fracture zone *2* of P1, as expected. Its continuation has not (yet?) reached P2 but it seems to be going in the direction of its fracture zone *2* (Figs. 3 and 4) although it is not at all parallel to the scarp of the landslide. There is no visible fracture in fracture zones *1*, neither in P1 nor in P2. These zones are special because they are at the edge of the landslide.

Figure 4 presents the correlation between the actual topography along P1 and P2 and their resistivity images. There are also two smaller fractures on P1 with vertical offsets of 0.4 and 0.2 m. These fractures were not predicted

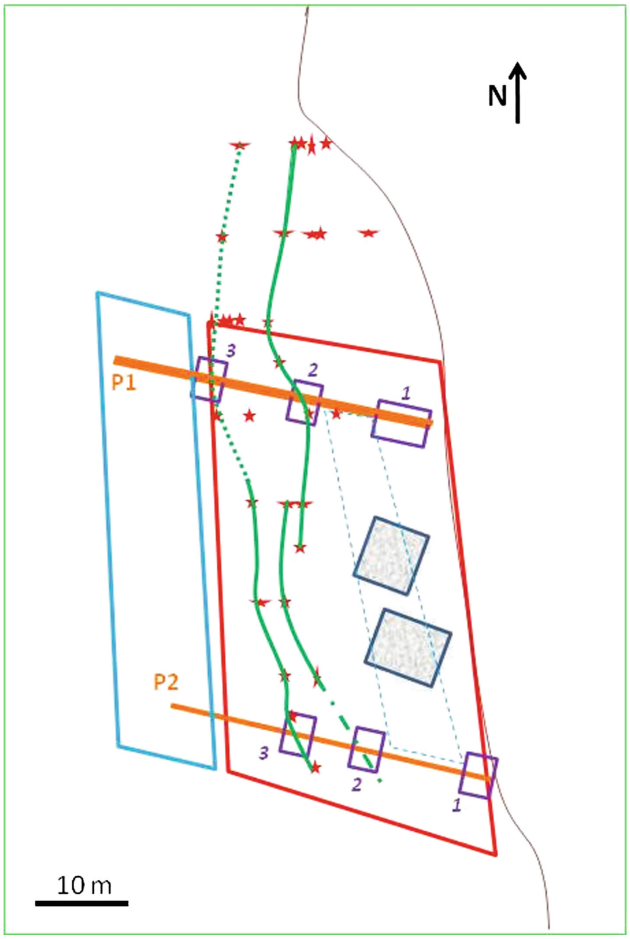

Fig. 5 Verification of the results (taken from Fig. 3). ERT profiles P1 and P2 (*brown lines*); the main fracture visible at the time of the measurements (*green dotted curve*); new fractures developed after the measurements (*green curves*); predicted continuation of the new fracture in the future (*point-dotted green curve*); the actual scarp (*thin brown curve*); actual fracture positions (*stars*); fracture zones which have been interpreted from the ERT results (numbered *violet rectangles*). Area assumed to be endangered (*red rectangle*); probably not yet endangered area (*blue rectangle*). Probably safe area inside of the dangerous one (*blue dotted line rectangle*). Ground-plan of the buildings (*filled rectangles*). The *light green rectangle* shows the same area as in Fig. 3

by our measurements. Most likely at the time of our measurements they did not exist yet. They must have been produced by the movement along the large fractures.

P3 is still free of visible fractures as expected. Because the part of the endangered area where there are houses seemed to be fracture-free, it was expected that they will not be severely damaged or destroyed. There is no fracture on the walls of the buildings which sank about 2 m without serious damage. All of our predictions have been verified by the mass movements of the last few months disregarding only from the small features below P1 which are assumed to have developed meantime due to the displacement along the predicted large fractures.

Conclusions

A slowly moving loess landslide was investigated using the ERT method. We focussed the study on its fracture system to determine its mechanically weak zones. It was expected that this knowledge will enable us to understand the process of mass movement and to forecast its future development. Mapping of the furthest significant fracture (zone) from the actual sliding front was expected to enable us to delineate the endangered area.

The field conditions were favourable in the study area because it is rather homogeneous and the top of the fractures are in only 5–10 cm depth. The investigation of such a dense fracture system, where the mean distance of the fractures is only about 0.5 m, may be difficult. The use of the ERT method to map such a fracture network was studied by numerical modelling and the results have been verified in the field. It was shown that:

1. It is better to carry out field measurements following dry periods.
2. The fractures have to be localised taking into account the anomalies at a depth where the near-surface artefacts disappear while the anomalies due to fractures are still well visible.
3. Fractures were also detectable in the field but they could mostly be followed only to a depth of about 1–2 m. Their surface projection could be mapped fulfilling the principal aims of the study.
4. The fractures are most easily detectable and separable if they are at about the same depth.
5. ERT was able to separate fracture zones and even many individual fractures rather well in the study area. Spacing electrodes 0.5 m apart, even fractures 0.4 m apart were separable.

In the study area the fractures and fracture zones appeared in the middle layer, at a depth of 0.5–1 m. We predicted that future mass movements are going to happen in these fracture zones. Therefore we stated (Fig. 5) that

1. The already visible MF will continue along fracture zone 3 in P2.
2. In fracture zone 2, a new rupture surface will open in P1.
3. The same was expected in fracture zone 2 in P2.
4. Blocks at the edge of the landslide (fracture zone 1 on P1 and P2) could separate at anytime.
5. Only the area east of zone 3 is endangered inside of the area between P1 and P2. The area west of this zone and the one below P3 is not yet endangered.
6. The area inside the endangered one (see point 5) where there are buildings may remain in one unit because it is fracture-free.

Expectations 1, 2, 5 and 6 have been verified by the mass movements one and a half years after the measurements. Expectation 3 has not yet been verified but regarding the actual situation of the new large fracture which is going through zone 2 on P2, it may be expected in the future. Expectation 4 has not been verified yet, but regarding earlier rupture surfaces it can easily take place. Only the smaller rupture surfaces could not have been predicted since they might have occurred during the mass movements along the larger surfaces.

By monitoring the changes in a landslide area, one can give an early risk warning using the ERT method to avoid damage to buildings or even danger to human lives.

References

Bai MZ, Du YQ, Kuang X (2012) Warning method and system in risk management for loess engineering slopes. J Perform Constr Facil 26 (2):190–196

Bányai L, Újvári G, Gy Mentes, Kovács M, Czap Z, Gribovszki K, Papp G (2013) Recurrent landsliding of a high bank at Dunaszekcső, Hungary: geodetic deformation monitoring and finite element modeling. Geomorphology 210:1–13

Bièvre G, Jongmans D, Winiarski T, Zumbo V (2012) Application of geophysical measurements for assessing the role of fissures in water infiltration within a clay landslide (Trieves area, French Alps). Hydrol Process 26:2128–2142

Booth AM, Roering JJ, Perron JT (2009) Automated landslide mapping using spectral analysis and high-resolution topographic data: Puget Sound lowlands, Washington, and Portland Hills, Oregon. Geomorphology 109:132–147

Caicedo B, Murillo C, Hoyos L, Colmeranes JE, Berdugo, IR (2013) Advances in unsaturated soils. Taylor and Francis Group, London, pp 165–169. ISBN 978-0-415-62095-6

Cruden DM, Varnes DJ (1996) Landslide types and processes, special report, transportation research board. Natl Acad Sci 247:36–75

Fábián SZÁ, Kovács J, Lóczy D, Schweitzer F, Varga G, Babák K, Lampért K, Nagy A (2006) Geomorphologic hazards in the Carpathian foreland, Tolna County (Hungary). Studia Geomorphologica Carpatho-Balcanica 40:107–118

Falco P, Negro F, Szalai S, Milnes E (2013) Fracture characterisation using geoelectric null-arrays. J Appl Geophys 93:33–42

Gallet S, Jahn B, Van Vliet Lanoe B, Dia A, Rossello E (1998) Loess geochemistry and its implications for particle origin and composition of the upper continental crust. Earth Planet Sci Lett 156: 157–172

Guzzetti F, Mondini AC, Cardinali M, Fiorucci F, Santangelo M, Chang K (2012) Landslide inventory maps: new tools for an old problem. Earth Sci Rev 112(1–2):42–66

Haase D, Fink J, Haase G, Ruske R, Pécsi M, Richter H, Altermann M, Jaeger KD (2007) Loess in Europe—its spatial distribution based on a European Loess Map, scale 1:2,500,000. Quatern Sci Rev 26:1301–1312

Highland L (2004) Landslide types and processes. https://pubs.usgs.gov/fs/2004/3072/pdf/fs2004-3072.pdf

Jones G, Sentanac P, Zielinski M (2014) Desiccation cracking using 2-D and 3-D electrical resistivity tomography: validation on a flood embankment. J Appl Geophys 106:196–211

Jongmans D, Garambois S (2007) Geophysical investigation of landslides: a review. Bull Soc Géol Fr 33:101–112

Lapenna V, Lorenzo P, Perrone A, Piscitelli S, Rizzo E, Sdao F (2005) 2D electrical resistivity imaging of some complex landslides in Lucanian Apennine chain, southern Italy. Geophysics 70:B11–B18

Li P, Zhang B, Li TL (2012) Study on regionalization for characteristic and destruction rule of slope in loess plateau. J Earth Sci Environ 34 (3):89–98 (In Chinese)

Liao HJ, Su LJ, Li ZD, Pan YB, Fukuoka H (2008) Testing study on the strength and deformation characteristics of soil in loess landslides. In: Chen Zuyu, Jianmin Z, Zhongkui L, Faquan W, Ken H (eds) Landslides and engineered slopes (from the past to the future). CRC Press, Leiden, vol 1, pp 443–447

Loke M, Chambers J, Rucker D, Kuras O, Wilkinson P (2013) Recent developments in the direct current geoelectrical imaging method. J Appl Geophys 95:135–156

Moyzes A, Gy Scheuer (1978) Engineering geological investigation of the high bank at Dunaszekcső. Földtani Közlöny 108:213–226

Pécsi M (1994) A landslide type occurring frequently along the loess bluff in the Hungarian Danube section. Quatern Int 24:31–33

Rónai A (1985) The quaternary of the Great Hungarian Plain. In: Pécsi M (ed) Loess and the quaternary. Akadémiai Kiadó, Budapest, pp 51–63

Scaioni M, Longoni L, Melillo V, Papini M (2014) Review. remote sensing for landslide investigations: an overview of recent achievements and perspectives. Remote Sens. 6. doi:10.3390/rs60x000x

Szalai S, Szarka L, Prácser E, Bosch F, Müller I, Turberg P (2002) Geoelectric mapping of near-surface karstic fractures by using null-arrays. Geophysics 67:1769–1778

Tofani V, Segoni S, Agostini A, Catani F, Casagli N (2013) Technical note: use of remote sensing for landslide studies in Europe. Nat Hazards Earth Syst Sci 13:299–309

Újvári G, Gy Mentes, Bányai L, Kraft J, Gyimóthy A, Kovács J (2009) Evolution of a bank failure along the River Danube at Dunaszekcső, Hungary. Geomorphology 109:197–209

Van Westen CJ (2004) Geo-Information tools for landslide risk assessment: an overview of recent developments. In: Proceedings of 9th international. symposium landslides, Rio de Janeiro, Brazil, Balkema, Rotterdam, pp 39–56